The Astronomical Journal, 127:3642–3652, 2004 June

DOME-DIFFUSER FLAT-FIELDING FOR SCHMIDT TELESCOPES

Xu Zhou,[1] David Burstein,[2] Yong-Ik Byun,[3] Jian-Sheng Chen,[1] Wen-Ping Chen,[4] Zhao-Ji Jiang,[1] Jun Ma,[1] Wei-Hsin Sun,[4] Rogier A. Windhorst,[2] Hong Wu,[1] Wen Xu,[1] and Jin Zhu[1]

Received 2003 August 5; accepted 2004 January 27

ABSTRACT

The Beijing-Arizona-Taiwan-Connecticut Color Survey of the Sky employs the 0.6/0.9 m Schmidt telescope of the National Astronomical Observatories, located at its Xinglong station (150 km northeast of Beijing), combined with a 2048^2 CCD data-taking system. Key to the success of this program is the development of a simple and efficient way to achieve supersky-quality, large-scale flat fields for our telescope-CCD combination. This is done by placing an isotropic diffuser right in front of the Schmidt corrector plate (the entrance pupil of the telescope) and illuminating the diffuser with scattered light off the dome screen. When we test this methodology by obtaining supersky flats at the zenith, we find that our "super" dome flats define the same large-scale inhomogeneities of the CCD that the supersky flat does, but with far greater signal-to-noise ratio. Hence, we show that defining our large-scale flat fields with our diffuser-dome technique is at least as good as using supersky flats for a $\sim 1^\circ$-wide field of view. This methodology can be implemented with any Schmidt telescope with similar results. Various other data acquisition effects that can affect CCD results at the 1% level are also discussed.

Key words: instrumentation: detectors — techniques: photometric

1. INTRODUCTION

The flat field of a CCD in an imaging camera located at the focal plane of a telescope can be defined to be the large-scale, two-dimensional response of that CCD to a source of uniformly distributed light that passes through the same optical system used to take images of the sky. In turn, the CCD flat field is the product of the two-dimensional variation of CCD quantum efficiency and the optical transfer efficiency, including telescope, filter, etc.

If the field of view of a typical CCD in a typical telescope camera covers $\sim 5'-10'$ on the sky, the sky is flat enough over those small size scales to provide an adequate source of nearly uniform illumination that satisfies the criteria for providing the flat field of a CCD. As such, astronomers have generally developed the habit of constructing "supersky" flats from their many exposures in a given filter taken during the night to define the flat fields of their CCDs. For most astronomers, the night sky has become the final arbiter of the flatness of their CCD images.

The situation is very different for those CCD systems in which an individual CCD covers more than $30'$ of the sky. Anyone who has looked carefully at the night sky realizes that on $\frac{1}{2}^\circ$ size scales (i.e., the size of the full Moon), the night sky is not uniform anywhere (see, e.g., Zheng et al. 1999; Morrison, Boroson, & Harding 1994; Walker 1987). The Beijing-Arizona-Taiwan-Connecticut (BATC) collaboration uses the 0.6/0.9 m f/3 Schmidt telescope of the National Astronomical Observatories, combined with a 2048^2 CCD located in its focal plane, to obtain nearly 1°-sized images of the sky in 15 intermediate filter bands (see Fan et al. 1996). In this configuration, the field of view of this one CCD subtends $58'$ of the sky.

Our survey includes large galaxies for which a 1° field of view is ideal for observing (see Shang et al. 1998; Zheng et al. 1999; Wu et al. 2002), as well as large-scale measures of stars and background galaxies in our field of view. As such, it was important for our survey to develop an alternate means of providing an accurate, high signal-to-noise ratio (S/N) flat field for our CCD system. Fortunately, the special characteristics of a Schmidt telescope permit one to develop a method by which dome flats can provide a very uniform source of illumination of our CCD. Specifically, placing a diffuser screen at the entrance pupil of the Schmidt telescope turns input radiation from a nearby source of light (such as a light in the dome) into isotropic input, such that the CCD camera inside the closed Schmidt telescope tube is very uniformly illuminated. As Fan et al. (1996), Shang et al. (1998), Zheng et al. (1999), and Wu et al. (2002) show empirically, this method of CCD flat-fielding provides very uniform images.

The purpose of the present paper is to detail the accuracy of the diffuser-related methodology that our flat fields employ. Section 2 introduces our equipment and our dome-diffuser flat-field method. The theoretical basis of the method is given in § 3, and a summary of the tests we have performed to show the efficacy of this method is given in § 4. Various additional factors that can also affect the flat-field correction are discussed in § 5. We present our conclusions in § 6.

2. EQUIPMENT AND METHODOLOGY

The f/3, 0.6/0.9 m Schmidt telescope is located at the Xinglong observing site of the National Astronomical Observatories of China (NAOC). The Xinglong site is some 150 km northeast of Beijing. The focal plane of the telescope has been equipped with a CCD dewar that contains a 2048^2 Ford Aerospace CCD, which uses the data-taking system designed by Lick Observatory. The BATC survey employs 15 intermediate-band filters specially designed to avoid the brighter night-sky lines from 3300 Å to 1 μm. These 15 filters are housed in a "typewriter style" arrangement around the inner

[1] National Astronomical Observatories, Chinese Academy of Sciences, 20A Datun Road, 100012 Beijing, China; zhouxu@bac.pku.edu.cn.
[2] Department of Physics and Astronomy, P.O. Box 871504, Arizona State University, Tempe, AZ 85287.
[3] Yonsei University Observatory, 134 Sinchon-dong, Seodaemun-gu, Seoul 120-749, Korea.
[4] Institute of Astronomy, National Central University, 32054 Chung-Li, Taiwan.

circumference of the Schmidt tube. Each filter is housed at one end of each "type bar." Computers control telescope pointing, camera operation, and placing and removing a filter arm from in front of the CCD camera.

The "typewriter"–CCD camera system is designed to provide a very snug and accurately reproducible fit between each filter and the CCD camera. The 2048^2 CCD has 15 μm pixels, which, combined with the intermediate-band filters, yield a plate scale of $1''.70$ pixel^{-1}. In this configuration, the camera subtends a solid angle of the sky of $58'$. As the average seeing at the Xinglong site (altitude 900 m) is $2''$–$3''$, the data taken by our CCD system are typically slightly undersampled (see, e.g., Fan et al. 1996).

The CCD camera system is presently being upgraded to permit CCD dewars to be easily put into the focal plane of the telescope. This will permit easier interchange of dewars containing thick and thin CCD chips, so observations with this telescope can make maximal use of these CCDs. For the present tests, a thick Ford Aerospace CCD was employed, UV-coated to give a quantum efficiency of ~18% in the UV and a peak efficiency of 40% at 7000 Å.

Our dome-diffusing system employs a sheet of translucent plastic, 0.6 m in diameter, to form a diffuser plate. This diffuser plate is designed to be easily mounted in front of the correcting plate of the Schmidt telescope, which itself defines the front end of the Schmidt tube. An illuminated dome screen is used as the primary source of input light for the diffuser plate for the flat fields taken for the BATC program.

3. THEORY

Assume that the field center of a CCD in the focal plane of a Schmidt telescope points to a given sky direction. Then a pixel at position (R, C) of the CCD corresponds to a given direction $\Omega(R, C)$. Consider a wave front at the entrance pupil of the Schmidt telescope optics, that is, incident on the corrector plate. The photons in this wave front that arrive at the position (R, C) of the CCD in the focal plane come from an areal integration over the entire entrance pupil of all photons coming from direction $\Omega(R, C)$:

$$\iint J(\Omega, x, y) T(\Omega, x, y) dx\, dy, \tag{1}$$

where $J(\Omega, x, y)$ is the light intensity of the wave front at position (x, y) (the spatial position in the plane of the telescope entrance pupil) along the direction Ω and $T(\Omega, x, y)$ is the transfer function of the optical system. The CCD response is then given by

$$\text{response}(R, C) = \text{QE}(R, C) \iint J(\Omega, x, y) T(\Omega, x, y) dx\, dy. \tag{2}$$

Here $\text{QE}(R, C)$ is the CCD quantum efficiency. If light comes from an area of uniformly bright sky,

$$J(\Omega, x, y) = \text{const}. \tag{3}$$

Equation (4) defines a CCD flat-field function, $\text{Flat}(R, C)$:

$$\text{Flat}(R, C) = k\, \text{QE}(R, C) \iint T(\Omega, x, y) dx\, dy. \tag{4}$$

In the ideal case, the telescope transfer function becomes

$$T(\Omega, x, y) = 1, \tag{5}$$

yielding a function $\text{Flat}(R, C)$ that is uniquely determined by the CCD quantum efficiency:

$$\text{Flat}(R, C) = k\, \text{QE}(R, C) \tag{6}$$

with k a normalization constant. For this ideal case, a light source of isotropic radiation at the entrance pupil, that is,

$$J(\Omega, x, y) = J(x, y) = \text{const}, \tag{7}$$

can produce exactly the same effect on the CCD as a fully uniform sky does:

$$\begin{aligned} \text{response}(R, C) &= \text{QE}(R, C) \iint J(\Omega, x, y) T(\Omega, x, y) dx\, dy \\ &= \text{const} \times \text{QE}(R, C) \\ &= \text{const} \times \text{Flat}(R, C). \end{aligned} \tag{8}$$

The only condition used for the above equality is that the areal integration over the entrance pupil be the same for all pixel positions (R, C) on the CCD. This condition can be satisfied if the isotropic light source is placed at the entrance pupil of the optical system. For a Schmidt telescope system, the entrance pupil is its correcting lens; hence, a diffuser plate placed directly in front of the Schmidt corrector lens acts as part of the entrance pupil.

In general, the condition $T(\Omega, x, y) = 1$ is not satisfied for any telescope optical system. Even the condition $T(\Omega, x, y) = T(x, y)$ is not satisfied. This is because the transfer function of the integral optical system varies as a consequence of internal obscuration and the reflecting and transmitting efficiencies of the optical elements. In such a case, an isotropic diffuser placed in front of the corrector lens can no longer produce exactly the same result as produced by a uniform sky. This case is discussed below and in the Appendix. However, we also note that a "uniform night sky" does not exist over degree-sized scales.

4. TESTS OF THE UNIFORMITY OF THE DOME-DIFFUSER CCD FLAT FIELD

4.1. *Zenith Supersky Flats versus Diffuse Superdome Flats*

The one direction in the sky for which the night-sky variation with altitude is both minimized and radially symmetric over ~1° size scales is obviously the zenith. If one takes the time during a photometric, moonless night to obtain a long series of sky-dominated images pointing straight at the zenith, one can minimize the effects of the nonuniformity of the night sky. However, very few (if any) astronomers take out a large fraction of their observing time to accumulate hours of integration pointing at their local zenith. Rather, the typical "supersky" is obtained by combining images of the sky (usually images taken for the scientific program in question) oriented at random directions and altitudes, and possibly contaminated by whatever moonlight is around.

To demonstrate how well our diffuse superdome flats correspond to supersky flats, two moonless nights of observation with the BATC 6660 Å filter were used to take supersky flats at the zenith. One set of images was taken on 2000 October 25 and the other taken on 2000 October 31. The sky flats for these two observing runs consist of 28 and 21 images, each of 600 s exposure, respectively. All bright stars are masked in each image, yielding an average of about 430 and 550 counts pixel^{-1} for these two nights, respectively. The supersky flats for each night's observations were obtained using IRAF.

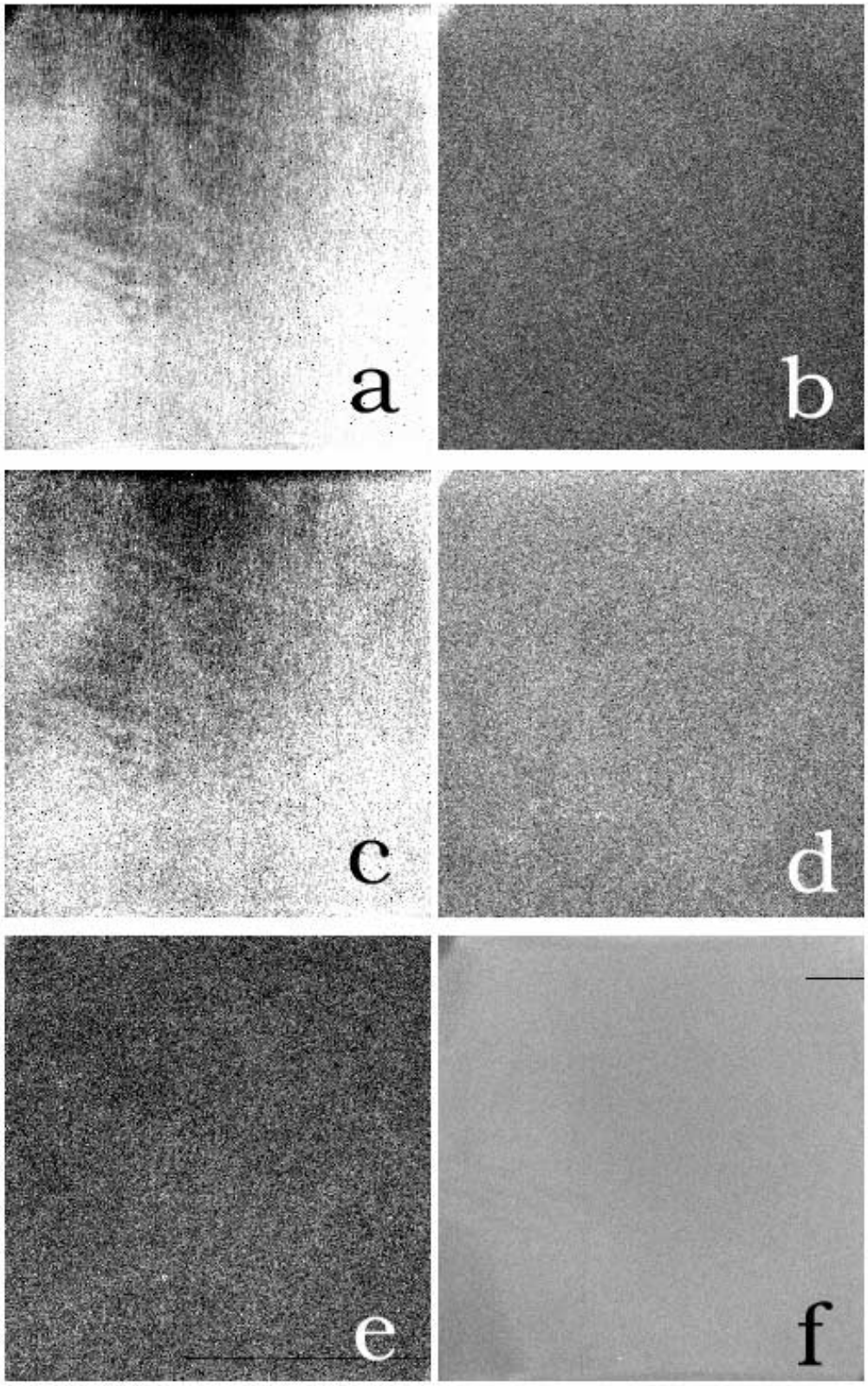

FIG. 1.—Montage of supersky flats and diffuser-dome flats from the two runs, all given at the same stretch (±5% from the mean). (*a*, *c*) Original flat-field images obtained with the dome diffuser and with the supersky flat for the first of our two observing runs. (*b*, *d*) Supersky flats from the two observing runs divided by the diffuser-dome flat of same run. Note how well the features seen in (*a*) and (*c*) are removed in this division. (*e*) Ratio of the two supersky flats. (*f*) Ratio of the two diffuser-dome flats. Note how stable the image is over a 6 day period.

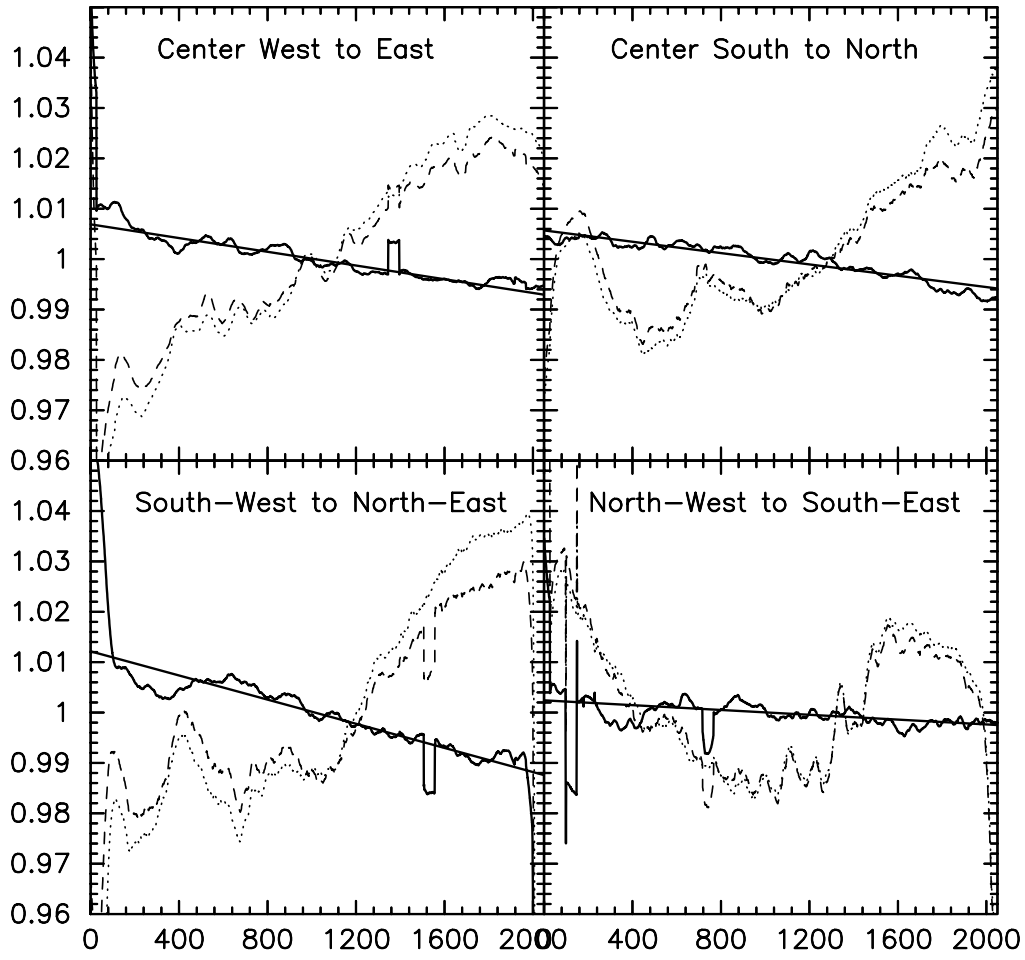

FIG. 2.—Four cuts across the image presented in Fig. 1*b* (division of supersky flat by dome-diffuser flat from the first observing run): along the middle row (west to east, *top left*); along the middle column (south to north, *top right*); southwest to northeast (*bottom left*); and northwest to southeast (*bottom right*). The small-scale noise in Fig. 1*b* is due to the poorer S/N of the supersky image. Excluding edge effects, the supersky/diffuser-dome ratio image has a residual intensity gradient of less than 1% from center to edge. For comparison, the same cuts across Fig. 1*a* (the original dome-diffuser flat) and Fig. 1*b* (the original supersky flat) are given (*dashed and dotted lines, respectively*).

Separately, for both nights we also took diffuser-dome flats, as is typical of our mode of observation. As with the supersky flats, the separate dome flats are combined to produce a "super" dome flat with an average of 10^6 counts pixel^{-1}, permitting pixel-to-pixel flat-fielding to have an accuracy of 0.1%.

Figure 1 shows these supersky and superdome flats in their original forms, as well as divided by each other. These images are shown at the same image stretch (±5% from the mean) to emphasize the structure in them. As is evident, both the supersky flat and the superdome flat are measuring the same large-scale flat field of the CCD. Figures 2–5 give cuts made through Figure 1*b* (Fig. 2), Figure 1*d* (Fig. 3), Figure 1*e* (Fig. 4), and Figure 1*f* (Fig. 5). These cuts demonstrate how closely the large-scale inhomogeneities in the CCD are matched by the supersky flat and the superdome flat, as well as the reproducibility of both the supersky flats and the superdome flats. In all figures, we show the same cuts through the original supersky and superdome flat images, again to show how well these flat fields correspond to each other.

It is evident from Figures 1–5 that the superdome flats taken with the translucent diffuser plate in front of the Schmidt corrector lens produce as flat an image of this CCD as do the supersky flats taken at the zenith. Ignoring edge effects in the CCD, one can see that both the zenith-based supersky flats and the dome-diffuser flats reproduce the CCD flat field to a mutual accuracy of ±1.2%. The largest gradient seen is in the southwest-to-northeast direction. As can be seen in Figure 4, the division of the two supersky flats shows gradients of ∼1% across the CCD in all four directions. In contrast, the division of the two superdome flats shows a gradient of ∼1% only in the northwest-southeast direction across the whole CCD. (Both estimates neglect edge effects in the CCD.) The gradients seen in the supersky-flat division are consistent with differences that occur in the night sky from night to night. In contrast, the superdome flat is more reproducible, in addition to providing a much higher S/N than any supersky flat.

At the least, our tests show that if we tried to obtain supersky flats only at the zenith for each filter for each night, we could not do better than we do by taking diffuser-dome flats for each filter during the day. Moreover, any supersky flat we could obtain would have significantly lower S/N that our superdome flats. This is why the papers the BATC team has published using this diffuser-dome flat technique have produced some of the most accurate large-scale flat images that exist in astronomy today (Fan et al. 1996; Shang et al. 1998; Zheng et al. 1999; Wu et al. 2002). It is with the diffuser-dome technology that we can routinely achieve ∼1% spectrophotometric

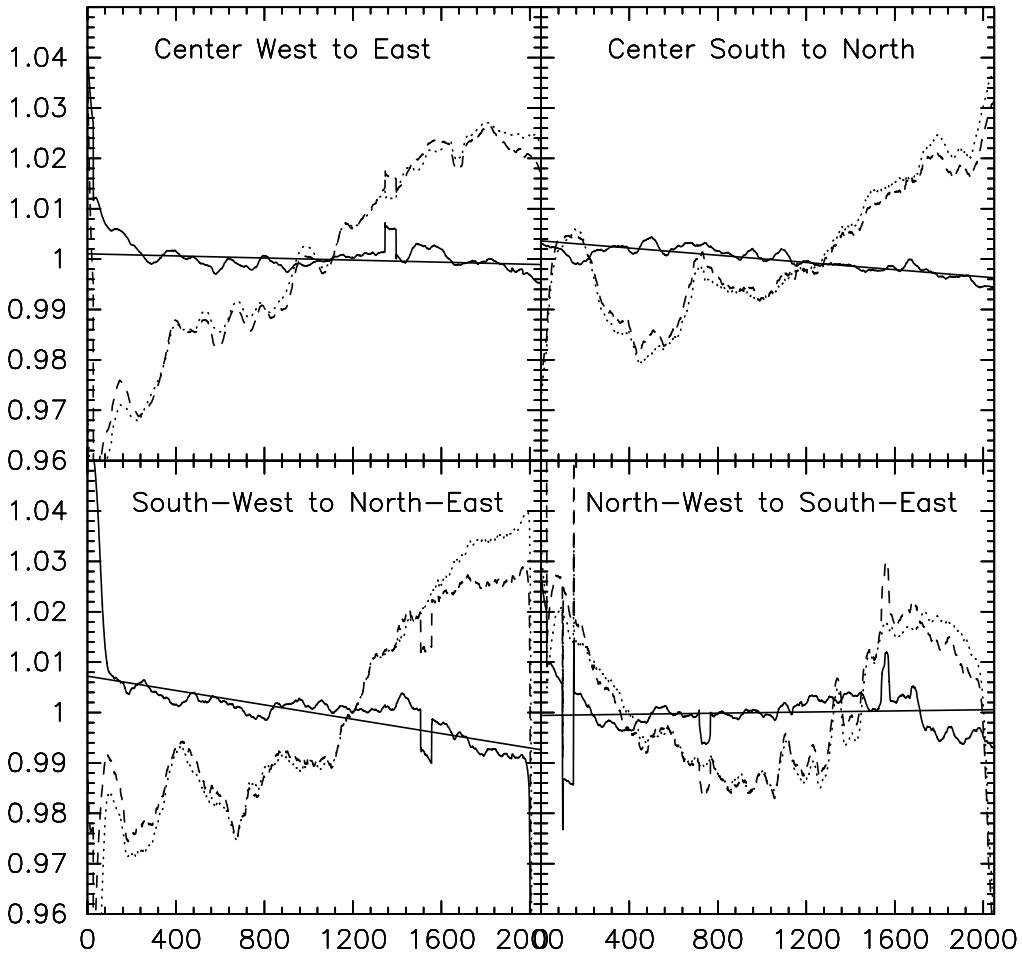

FIG. 3.—Cuts analogous to those of Fig. 2 across Fig. 1*d* (division of supersky flat by dome-diffuser flat for the second observing run). The meaning of the curves is the same as in Fig. 2. As with Fig. 1*b*, excluding edge effects, any residual intensity gradients are less than 1%. Figs. 1, 2, and 3 show that the dome-diffuser flat field is as reliable as the best supersky flat one can obtain.

accuracy with our CCD-plus-filter system (see also Yan et al. 2000).

4.2. *Comparison of Flats with and without the Diffuser*

It is also relevant to ask how well employing the diffuser increases the accuracy of the large-scale flat field one would get from just taking images of the dome screen without the diffuser in place. This test is done with separate flats from those discussed before. Figure 6 shows the image formed from the division of the flat using the diffuser relative to the flat not using the diffuser. Figure 7 is analogous to the cuts in Figures 2–5, showing how the division of the diffuser flat by the nondiffuser flat compares. As can be seen, the nonuniformity of the nondiffuser flat is over 2% over most of the CCD, rising to much higher values near the upper edge of the CCD (as shown in Fig. 6). It is clear that using the diffuser improves the large-scale flat field we would otherwise obtain by observing the dome flat without a diffuser in place.

4.3. *Degree of Isotropy of the Diffuser*

In the Appendix, we describe the effect of anisotropy of the incident radiation on the diffuser by simulating a special case (Fig. 8). Equation (A3) shows that the condition that radiation incident on the diffuser be isotropic makes the main part of the term ΔI vanish. This leads us to the question of how isotropic our diffuser plate can really be. A high degree of isotropy in the incident radiation is easy to achieve around the direction normal to the emitter. This is especially true if isotropy of the input light is required over only a small solid angle. For a CCD field size of $\sim 1^\circ$, a half-degree solid angle of input-light isotropy is needed around the normal direction to the diffuser plate. Obviously, the larger the angle from the normal direction, the more uniform a light source is required. Our tests indicate that for the existing dome source of radiation with our Schmidt telescope, we can achieve CCD flat fields from the diffuser that are isotropic at a level of 0.1%–0.5%, center to edge.

4.4. *Advantages of the Diffuser-Dome Flat-Field Method*

Our flat-field method has the advantage of the kind of high S/N normally associated with twilight flat fields, with the large-scale stability normally associated with supersky flat fields. In fact, our method provides as many photons per pixel as desired by the user. Without sacrificing nighttime observing, this is achieved by simply taking as many daytime dome flats as one desires. In practice, our survey would like our flat fields to be accurate to 0.1% or better, pixel to pixel. This means that each pixel needs 10^6 electrons. For CCD gain of 4, a saturated exposure produces about 10^5 e^- pixel^{-1}. In principle, 12 exposures are sufficient to yield S/N = 1000 pixel^{-1}. In practice, obtaining 50 dome-diffuser images during the daytime is easily accomplished, giving us flat fields of

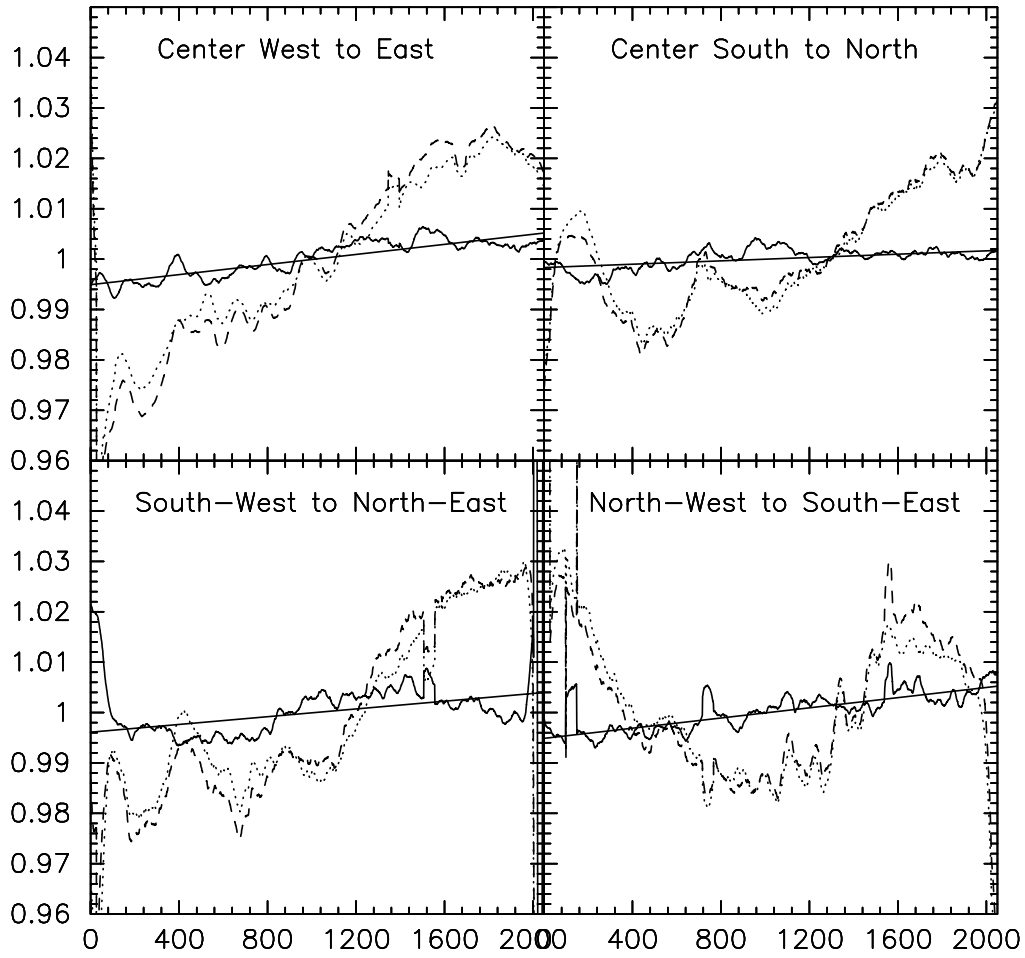

FIG. 4.—Cuts analogous to those of Fig. 2 across Fig. 1*e* (the division of the two supersky flats). The meaning of the curves is the same as in Fig. 2.

the requisite S/N for every night. Another advantage over the conventional flat-fielding method is that the data reduction of flat-field correction becomes straightforward. It just requires dividing the target images by the summed, averaged, dome-diffuser flat-field image.

5. OTHER IMPORTANT FACTORS AFFECTING THE FLAT-FIELD CORRECTION

5.1. *Factors Affecting the Flat Field*

5.1.1. *Color and Quantum Efficiency*

The quantum efficiency of a CCD varies from pixel to pixel as a function of the effective wavelength of incoming light. This makes an accurate flat-field correction difficult if the flat field is of a different effective wavelength than the program field. If we want to have a flat background for our program fields, the color temperature of the light source for the flat fields should be close to that of the night sky.

Yet, it is obvious that not all stars in the image will have the same color. As a result, it is the color dependence of CCD pixels that usually defines the accuracy limit for CCD photometry, to about 0.01 mag for broadband filters. However, the color effect is minimized if the effective wavelength of a filter changes little with the color of the incoming radiation. Such is the case for our intermediate-band filters, which are typically one-third to one-fifth the width of the broadband *UBVRI* filters.

Additional care should be taken to choose the dome lamp, dome reflecting screen, and diffuser transmission to match as closely as possible the color of the night sky. Such has been done for the dome-diffuser system with the NAOC Schmidt telescope. What we do notice is that, even with all the best choices made, we still observe less accuracy for filters with effective wavelengths shorter than 4500 Å. This may be due to a more complicated variation of CCD quantum efficiency at shorter wavelengths in our system and a stronger difference of the color temperature of the dome light from that of the night sky.

5.1.2. *Scattered Light and Filter Positioning*

A Schmidt telescope is an enclosed tube with the corrector plate as the light input into the telescope. The inside of the Xinglong Schmidt telescope is painted a rough black and has a reflectivity of less than 1%. As such, the effect of scattered light within this telescope is minimized, and certainly less than in a typical reflecting telescope.

When exposures are taken with twilight or dome illumination, scattered light that does not pass through the filter may directly reach the CCD. These scattered-light photons will obviously change the flat field. The situation becomes very serious when exposures are taken in the UV band, where the QE of our thick CCD is low. Fortunately, our multifilter system permits us to estimate the contribution of scattered light to our UV flat fields, as scattering of light occurs over the full

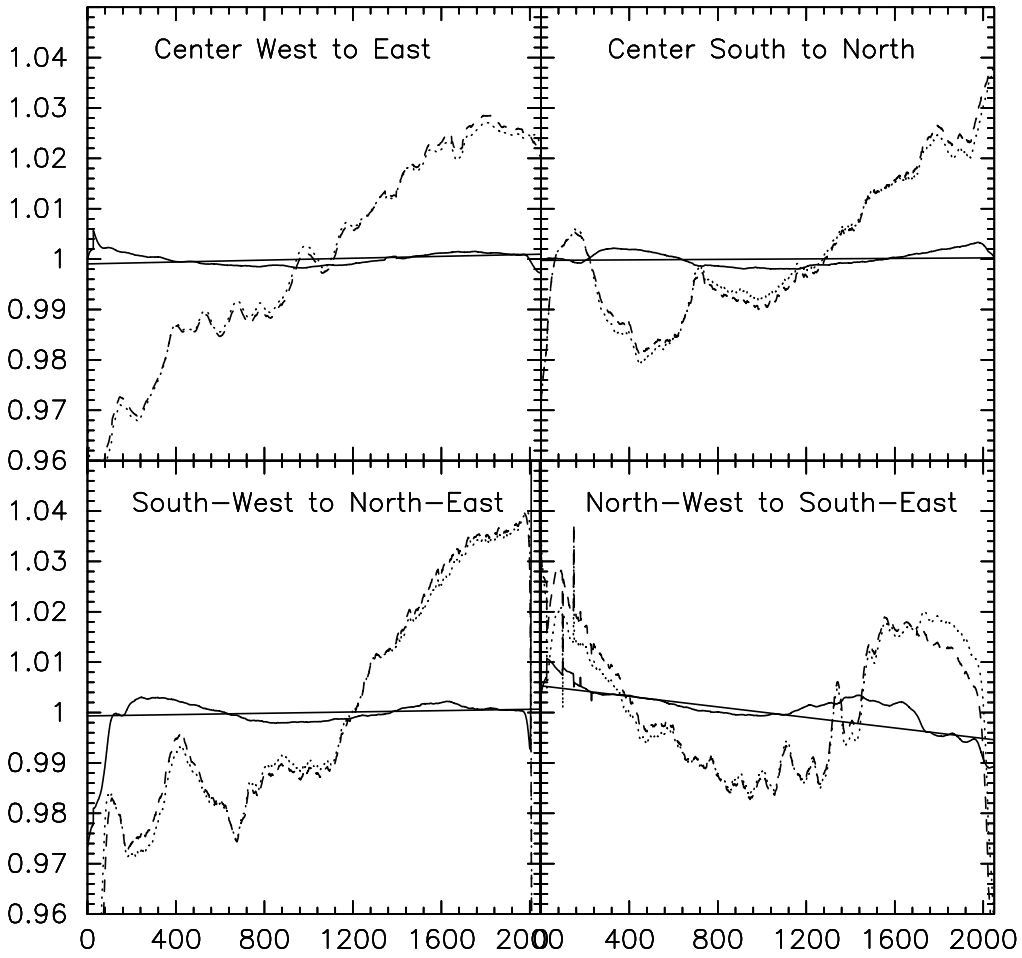

FIG. 5.—Cuts analogous to those of Fig. 2 across Fig. 1*f* (the division of the two superdome flats). The meaning of the curves is the same as in Fig. 2.

FIG. 6.—Image formed by the division of a flat field taken with the diffuser in place by a flat field taken without the diffuser in place. This test was done with separate flat fields from those used previously.

wavelength range, from the UV to the near-IR. On the other hand, the UV photons that arrive at the CCD through the filter are only a very small fraction of the total light coming through the diffuser. Putting all these factors together, even a scattered-light contribution of only 0.01% of the total incoming light can produce CCD ADU counts in the UV comparable to the CCD ADU counts of a real UV-band flat-field image.

Most conventional filter wheels have a gap between the filter and the CCD, which permits scattered light to affect the CCD. Such was the case in the original filter wheel used for the Schmidt telescope. One reason for going to the "type-writer style" filter holders described in § 2 was to have a filter holder that fit more snugly to the CCD. As a result, our filter-changing system has a special design that works like a box cover that does not permit any scattered light to enter the CCD. By our own tests, this has much improved the UV-band flat fields, to the point where their accuracy is similar to that of the 0.1%–0.5% seen with longer wavelength flat fields.

Any nonrepeatable positioning of filters, especially the interference filters used for our survey, will cause variation of the central wavelength, bandpass, etc. This is because the filter transmission is not absolutely constant over the whole face of the filter. Poor positioning of the interference filter would therefore affect the accuracy of our flat fields. This is why we designed our computer-controlled filter-changing system to work only when the filter is perfectly positioned. A special design for the mechanical system also ensures that the filter holder is guided into the correct position each time.

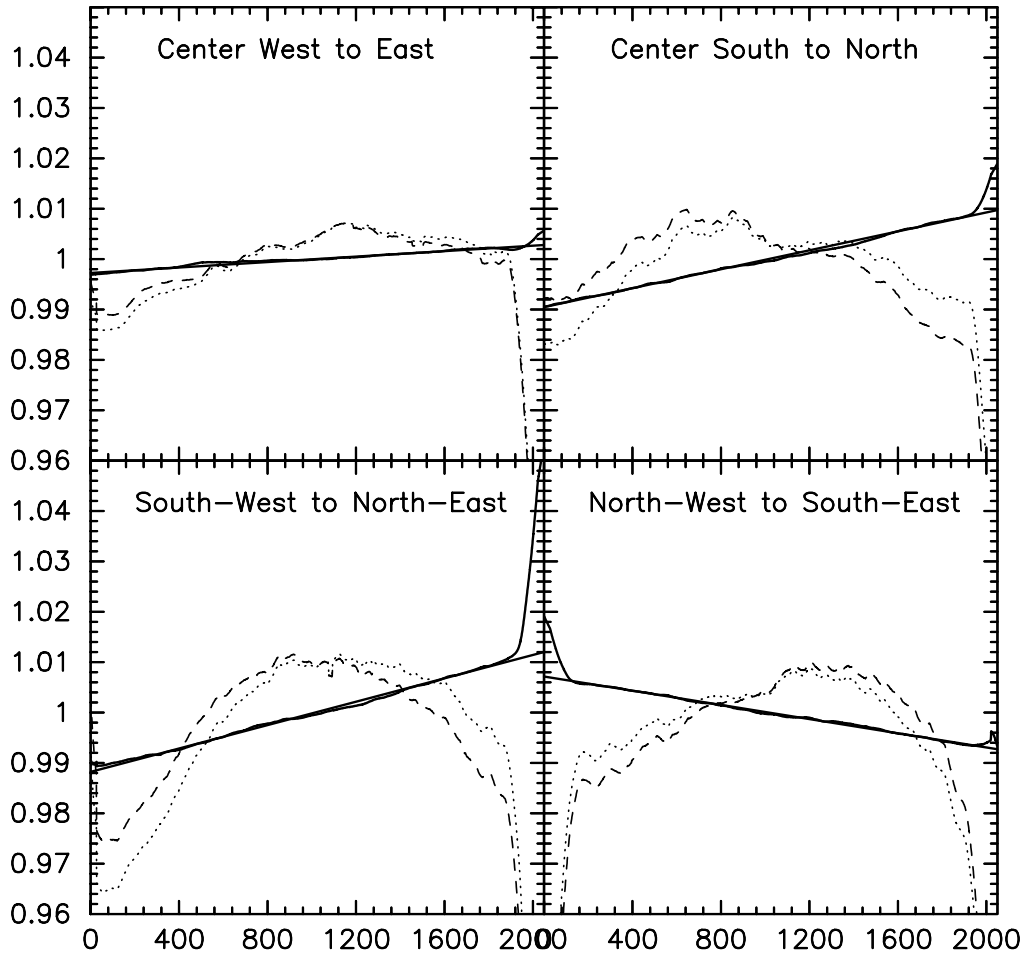

FIG. 7.—Cuts analogous to those of Fig. 2 across the image shown in Fig. 6. The meaning of the curves is the same as in Fig. 2.

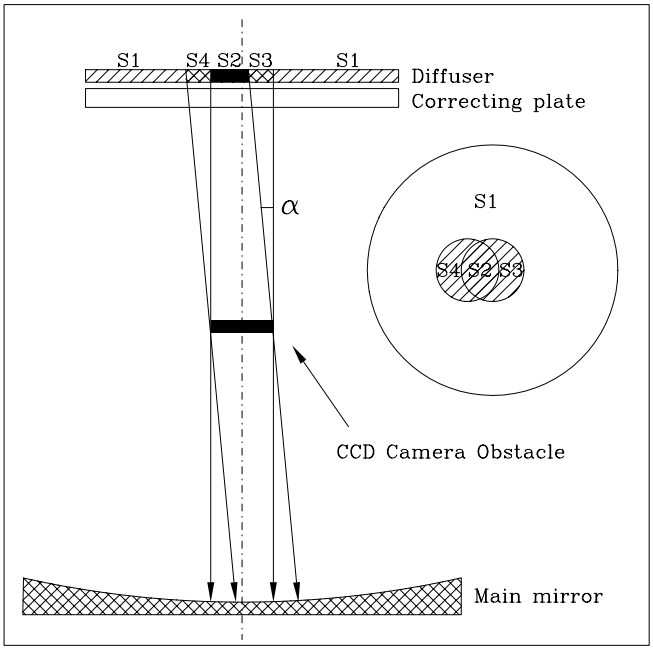

FIG. 8.—Two light paths together with the Schmidt optics. One light path goes to the CCD center and the other goes to the edge. The diffuser plane is divided into four parts, S_1, S_2, S_3, and S_4, corresponding to these two light paths.

5.1.3. *Shutter Effect*

Any CCD shutter opens and closes in a finite time. As the CCD shutter on our system is an iris shutter, the central part of the CCD is exposed for a longer time than the outer part of the CCD. Thus, the real exposure time for the CCD is pixel dependent, $T + \delta T(R, C)$, in a radial manner. The form of $\delta T(R, C)$ will be slightly different from exposure to exposure, and hence it cannot be predicted a priori. Empirical tests indicate the time to open and to close the shutter is $\sim$0.1 s, center to corner. If a 0.1% flat-field accuracy is required, the exposure time should therefore be longer than 100 s. Dome illumination of the diffuser plate can easily be adjusted to satisfy this requirement.

5.1.4. *Stability of CCD Flat Field*

Long-term changes have been noted with our CCD system, owing to the decay of the efficiency of the Lumigen UV-sensitive coating. As the Lumigen efficiency decays, the blue sensitivity of the CCD also decays, on a timescale of days. Our experiments show that the amplitude of the color temperature variation of the dome flat field is less than 0.0003 on a timescale of hours.

5.1.5. *CCD Temperature Effect*

If the cooling system of the CCD is not perfect, the CCD temperature can be modified by dome temperature. In a poor cooling system, the CCD temperature even can change with

the pointing direction of the telescope, the quantity of liquid nitrogen left in the dewar, etc. The variation of the two-dimensional distribution of temperature over the CCD will cause variation of the CCD quantum efficiency over the CCD and therefore cause variation of the CCD flat field. Our CCD system is constructed to minimize such effects. However, for future reference it is desirable to understand the behavior of CCD quantum efficiency variation with temperature variation.

5.2. *Dome Diffuser: Schmidt Telescope versus Standard Reflecting Telescope*

Can this method of flat-fielding be used with a standard reflecting telescope? The entrance pupil of a reflecting telescope is its main mirror. We cannot put the diffuser immediately in front of the main mirror, because then the diffuser will interrupt the light from the main mirror to the prime focus or to a secondary mirror (e.g., the Cassegrain focus). If we put the diffuser behind the prime focus or the second mirror, then the integrated area of light over the diffuser for different positions on the CCD is different. In those cases in which the CCD field used for large reflectors is only a few arcminutes, the difference in integrated area is not serious. We expect that the diffuser method can also produce good flat fields for most reflecting telescopes if the CCD field of view is small. However, the problem of scattered light remains for any telescope with an open-tube structure.

Conversely, every Schmidt telescope in astronomy could benefit in its CCD use by employing a diffuser plate to be placed right in front of the corrector lens. As we have shown here, by use of such a system Schmidt telescopes are turned into very accurate systems for determining large-scale properties of the night sky.

6. CONCLUSIONS

The observational goal of the Beijing-Arizona-Taiwan-Connecticut Color Survey of the Sky is to do 1% absolute spectrophotometry for all stellar and diffuse objects in our 58 arcmin^2 field of view, down to a limiting magnitude equivalent to $B = 21$. As we have already demonstrated (e.g., Fan et al. 1996; Shang et al. 1998; Zheng et al. 1999; Yan et al. 2000; Wu et al. 2002), our survey data are capable of reaching these goals.

In order to be able to perform 1% absolute spectrophotometry with a CCD system, much care must be given to all aspects of the data-taking and data reduction processes required to create a final data product. In the present paper we detail those parts of the data-taking process that are concerned with producing an output from the CCD that is as stable and clean as we can make it.

Chief among the methods developed by our team is the use of a translucent diffuser plate placed in front of the Schmidt corrector lens of our telescope to produce very reproducible, very flat, flat fields in each our 15 intermediate-band filters. In particular, we show that the conventional way of creating supersky flats, namely, combining images of the sky taken in random directions, yields a nonflat flat field on degree size scales, owing to the natural existence of altitude-dependent gradients in the night sky from the zenith to the horizon. As we demonstrate, even taking a super-supersky flat made of images all taken at the zenith does not do better than our diffuser–dome flat method of flat-fielding. The ability to use a dome flat system to take accurate flat fields means that we can observe up to eight of our BATC filters on a given night without the onus of obtaining supersky flats for any of the filter images.

Other CCD- and observing-related effects for which one must account in order to avoid introducing systematic effects larger than 1% into CCD data are also discussed. These factors include accuracy of filter positioning, minimizing scattered light, minimizing effects of finite CCD shutter speed, and having accurate CCD temperature control. However, it is the fact that CCDs have a color-dependent quantum efficiency that ultimately places the limit of 1% on the accuracy of the zero point of our CCD multicolor photometry.

We conclude by pointing out that this diffuser-dome method can be used to readily yield efficient flat fields with any Schmidt telescope equipped with a CCD data-taking system.

This project is supported by the Chinese Academy of Sciences, the Chinese National Natural Science Foundation, and the Chinese State Committee of Sciences and Technology. The US astronomers at Arizona State University and the University of Arizona have been supported in part by NSF grant INT 93-01805. In addition, we gratefully acknowledge support from our respective US universities (Arizona State University, the University of Arizona, and Western Connecticut State University), and we thank the referee for a careful reading of our paper.

APPENDIX

The special case in which there is obscuration in the light path of an optical system is considered here. Assume, as before, that any given pixel (R, C) at the CCD corresponds to a direction α, which defines where the light comes from. The light transmitted by an arbitrary element on the diffuser into a direction α can either arrive at pixel (R, C) of the CCD or be obstructed by mechanical elements, such as the CCD head, dewar, and mechanical supports. For a given incident direction α from the diffuser, we can always classify the area of the diffuser into two parts: Sa(α), the direction α of the incident unobstructed light that arrives at pixel (R, C), and Sb(α), the direction α in which light arrives at pixel (R, C) when that light is obstructed. We consider two pixels of the CCD, (R_1, C_1) and (R_2, C_2), corresponding to two incident directions α_1 and α_2, respectively. The area of the diffuser then can be classified into four parts:

S_1.—Light can arrive at pixels (R_1, C_1) and (R_2, C_2) from each incident direction, α_1 and α_2, respectively;

S_2.—No light from either direction α_1 or direction α_2 arrives at the CCD;

S_3.—Light can arrive at (R_1, C_1) from direction α_1 but cannot arrive at (R_2, C_2) from direction α_2; and

S_4.—Light can arrive at (R_2, C_2) from direction α_2 but cannot arrive at (R_1, C_1) from direction α_1.

The total light arriving at (R_1, C_1) is the integral of light over areas S_1 and S_3 and is

$$I_1 = \iint_{S_1+S_3} J(\alpha_1, x, y)dx\,dy. \tag{A1}$$

Similarly, the total light arriving at (R_2, C_2) is the integral of light over areas S_1 and S_4 and is

$$I_2 = \iint_{S_1+S_4} J(\alpha_2, x, y)dx\,dy. \tag{A2}$$

The difference between I_2 and I_1 is

$$\Delta I = I_2 - I_1 = \iint_{S_1} [J(\alpha_1, x, y) - J(\alpha_2, x, y)]dx\,dy + \iint_{S_4} J(\alpha_2, x, y)dx\,dy - \iint_{S_3} J(\alpha_1, x, y)dx\,dy. \tag{A3}$$

If the condition of *isotropic radiation* is satisfied,

$$J(\alpha_1, x, y) = J(\alpha_2, x, y) = J(x, y), \tag{A4}$$

then the first integral on the right-hand side of equation (A3) vanishes,

$$\Delta I = \iint_{S_4} J(x, y)dx\,dy - \iint_{S_3} J(x, y)dx\,dy. \tag{A5}$$

Defining $\delta I = \Delta I/I_1$ and rewriting $J(x, y)$ as

$$J(x, y) = J[1 + \eta(x, y)], \tag{A6}$$

we can write δI as follows:

$$\delta I = \frac{J\iint_{S_4}(1+\eta)dx\,dy - J\iint_{S_3}(1+\eta)dx\,dy}{J\iint_{S_1+S_3}(1+\eta)dx\,dy} = \frac{S_4 - S_3 + \iint_{S_4}\eta\,dx\,dy - \iint_{S_3}\eta\,dx\,dy}{S_1 + S_3 + \iint_{S_1+S_3}\eta\,dx\,dy}. \tag{A7}$$

Now consider light coming from two directions in a uniform sky and arriving at (R_1, C_1) and (R_2, C_2), respectively. The uniform brightness in the sky gives $\eta = 0$, and we have

$$\delta I_{\text{sky}} = \frac{S_4 - S_3}{S_1 + S_3}. \tag{A8}$$

The difference between the CCD flat field (determined by observing a uniform bright sky) and the flat field obtained by using a diffuser can be described by δ, the difference between δI and δI_{sky}:

$$\delta = \delta I - \delta I_{\text{sky}} = \frac{(S_1 + S_3)(\iint_{S_4}\eta\,dx\,dy - \iint_{S_3}\eta\,dx\,dy) - (S_4 - S_3)\iint_{S_1+S_3}\eta\,dx\,dy}{[(S_1 + S_3) + \iint_{S_1+S_3}\eta\,dx\,dy](S_1 + S_3)}. \tag{A9}$$

We can define $\langle\eta\rangle_{S_3}$, $\langle\eta\rangle_{S_4}$, and $\langle\eta\rangle_{S_1+S_3}$ as

$$\langle\eta\rangle_{S_3} = \frac{\iint_{S_3}\eta\,dx\,dy}{S_3}, \qquad \langle\eta\rangle_{S_4} = \frac{\iint_{S_4}\eta\,dx\,dy}{S_4}, \qquad \langle\eta\rangle_{S_1+S_3} = \frac{\iint_{S_1+S_3}\eta\,dx\,dy}{S_1 + S_3}. \tag{A10}$$

The quantity $\langle\eta\rangle$ measures the brightness fluctuation per unit area of the diffuser. Using these definitions (eq. [A10]), equation (A9) can be rewritten as

$$\delta = \frac{S_4\langle\eta\rangle_{S_4} - S_3\langle\eta\rangle_{S_3} - (S_4 - S_3)\langle\eta\rangle_{S_1+S_3}}{(S_1 + S_3)(1 + \langle\eta\rangle_{S_1+S_3})} = \frac{S_4(\langle\eta\rangle_{S_4} - \langle\eta\rangle_{S_1+S_3}) - S_3(\langle\eta\rangle_{S_3} - \langle\eta\rangle_{S_1+S_3})}{(S_1 + S_3)(1 + \langle\eta\rangle_{S_1+S_3})}. \tag{A11}$$

It is obvious that

$$\delta \le \frac{S_4\left|\langle\eta\rangle_{S_4}-\langle\eta\rangle_{S_1+S_3}\right| + S_3\left|\langle\eta\rangle_{S_3}-\langle\eta\rangle_{S_1+S_3}\right|}{(S_1+S_3)(1+\langle\eta\rangle_{S_1+S_3})} \le \frac{S_4+S_3}{S_1+S_3}\max\left(\frac{\left|\langle\eta\rangle_{S_4}-\langle\eta\rangle_{S_1+S_3}\right|}{1+\langle\eta\rangle_{S_1+S_3}}, \frac{\left|\langle\eta\rangle_{S_3}-\langle\eta\rangle_{S_1+S_3}\right|}{1+\langle\eta\rangle_{S_1+S_3}}\right). \tag{A12}$$

Therefore, we strictly have $\delta \le T\bar{\eta}$, where $T = (S_4 + S_3)/(S_1 + S_3)$ and $\bar{\eta}$ is defined as

$$\begin{aligned}\bar{\eta} &= \max\left(\frac{\left|\langle\eta\rangle_{S_4}-\langle\eta\rangle_{S_1+S_3}\right|}{1+\langle\eta\rangle_{S_1+S_3}}, \frac{\left|\langle\eta\rangle_{S_3}-\langle\eta\rangle_{S_1+S_3}\right|}{1+\langle\eta\rangle_{S_1+S_3}}\right)\\ &\le \frac{2}{1+\langle\eta\rangle_{S_1+S_3}}\max\left(\left|\langle\eta\rangle_{S_4}\right|, \left|\langle\eta\rangle_{S_3}\right|, \left|\langle\eta\rangle_{S_1+S_3}\right|\right) \le \frac{2}{1-\eta^{\max}}\eta^{\max},\end{aligned} \tag{A13}$$

where $\eta^{\max}$ is the maximum of $\eta(x, y)$. For the case of poor illumination of the diffuser, $\eta^{\max}$ could be as large as 10% of the mean intensity of the brightness of the diffuser, $\bar{\eta} \le 0.2$.

Let us consider a typical obscuration of the light path. A CCD camera is mounted at the center of the focal plane. The diameter of the camera is $d = 0.10$ m, the aperture of the telescope $D = 0.6$ m, and the focal length $f = 1.8$ m. We compare the δ for the worst case, in which one point is at the center of the CCD and the other is at one edge. The angle between the two paths is about half of the field of view, $\alpha = 0.^{\circ}5$. In this worst-case scenario (see Fig. 8), we find

$$S_1 = \frac{\pi}{4}(D^2 - d^2) \approx \frac{\pi}{4}D^2, \qquad S_3 \approx \frac{f\alpha d}{2}, \qquad T \approx \frac{4f\alpha d}{\pi D^2}.$$

If there is a 10% gradient in input radiation, plugging in the numbers yields $T \le 0.006$ and $\delta \le 0.0006$. Hence, the large-scale (e.g., from center to corner of the CCD) flat-field correction is accurate to 0.0006 or better for 10% fluctuations in the brightness distribution input to the diffuser.

REFERENCES

Fan, X., et al. 1996, AJ, 112, 628
Morrison, H. L., Boroson, T. A., & Harding, P. 1994, AJ, 108, 1191
Shang, Z., et al. 1998, ApJ, 504, L23
Walker, M. F. 1987, in Identification, Optimization, and Protection of Optical Telescope Sites, ed. R. L. Millis, O. G. Franz, H. D. Ables, & C. C. Dahn (Flagstaff: Lowell Obs.), 128
Wu, H., et al. 2002, AJ, 123, 1364
Yan, H. J., et al. 2000, PASP, 112, 691
Zheng, Z., et al. 1999, AJ, 117, 2757